Experimental visualization of the cathode layer in AC surface dielectric barrier discharge

Sang-You Kim, Taihyeop Lho, and Kyu-Sun Chung

Citation: Physics of Plasmas **25**, 064503 (2018); doi: 10.1063/1.5027794
View online: https://doi.org/10.1063/1.5027794
View Table of Contents: http://aip.scitation.org/toc/php/25/6
Published by the American Institute of Physics

Experimental visualization of the cathode layer in AC surface dielectric barrier discharge

Sang-You Kim,[1,a)] Taihyeop Lho,[2] and Kyu-Sun Chung[1]
[1]*Department of Electrical Engineering, Hanyang University, 04763 Seoul, South Korea*
[2]*Plasma Technology Research Center, National Fusion Research Institute, 54004 Gunsan, South Korea*

(Received 6 March 2018; accepted 23 May 2018; published online 7 June 2018)

A narrow etched polyimide line at the bottom edge of a biased electrode (BE) and a non-etched dielectric surface near the biased electrode were observed in an atmospheric AC flexible surface dielectric barrier discharge of polyimide dielectric. These findings are attributed to the bombardment of positive oxygen ions on the bottom edge of the BE and the electron breakdown trajectory not contacting the polyimide surface following the electric field lines formed between the BE edge and the surface charge layer on the dielectric. The length of the non-etched dielectric surface during the first micro-discharge was observed as 22 μm. This occurred, regardless of three different operating durations, which is in good agreement with the length of the cathode layer according to Paschen's law. *Published by AIP Publishing.*
https://doi.org/10.1063/1.5027794

A surface dielectric barrier discharge (SDBD) has a simple structure of one small electrode as the biased electrode (BE) on a dielectric surface and large electrode as the ground electrode (GE) on its reverse side.[1,2] When a high voltage AC or pulse is applied to a BE, many micro-discharges are generated near the edge of the BE, and they develop along the dielectric surface.[1–3] Since air flows around the SDBD can be controlled by momentum exchanges between negative oxygen ions in micro-discharges and molecules in air, the SDBD has been widely researched as a plasma actuator in aerodynamics.[1,3–6]

Various fluids and kinetics models have been proposed for explaining the experimental results in SDBDs.[5–8] Some experimental reports have shown that they are in agreement with the macroscopic characteristics such as the length of discharge region, streamer development,[8–10] and electrohydrodynamic (EHD) force.[6] Electrical breakdown, positive charges distribution, secondary electron emission from the BE, and its avalanche for ion-electron breeding can be modeled by the formation of a cathode layer.[1,2,7,8,11,12] However, because the thickness of the cathode layer at 760 Torr is about 20 μm according to Paschen's law,[1] the presence of a cathode layer has not yet been experimentally verified. Figures 1(a)–1(d) show the formation of "the gap" near to the BE and sustaining micro-discharges by ion-electron breeding during the first phase of negative polarity[1,8] by comparing the pristine surface [Figure 1(a)] with those of damaged ones [Figs. 1(b)–1(d)].

Positive ions (O_2^+),[13,14] oxygen atoms (O),[13–15] ozone (O_3),[15] and metastable oxygen molecules (O_2^*)[16] etch polyimide (PI) in all ranges of pressure by various physical and chemical processes.[13,14] An important role is played by O_2^+ in etching polyimide by chemically enhanced physical sputtering, surface-damage-promoted etching, chemical sputtering by supplying surface energy, and direct reactive ion etching. The oxygen atoms produced by electron-impact dissociation of O_2 molecules,[17] and the recombination process of O_2^+ and electrons are also significant in etching PI in SDBDs.[3,7,17,18]

In the atmospheric SDBDs, O_2^+ is created inside a cathode layer[1,7,8,11] by an electron avalanche and the above dielectric by photo-ionization from reactive nitrogen species[7,19] during the negative voltage phase, and inside streamers during the positive voltage phase. The recombination process that creates O for etching PI occurs where the micro-discharges containing electrons make contact with PI. Therefore, O in SDBD has a high selectivity[20] in etching PI due to sharp increases with a reduced electric field (E/N),[17] the formation of floating potential on the PI, and its essential exothermic reaction. This reaction can be clearly distinguished from other PI etching caused by electrically neutral $O_2^*(a^1\Delta_g$ and $b^1\Sigma_g^+)$.[3,16] Due to the slow formation of ozone,[21] most of the oxygen atoms created on the PI could etch the PI without the contribution of ozone formation. Although the negative oxygen ions (O_2^-, O_3^-) can also etch PI, they have rare participation in etching PI due to recombination with the positive ions and their repulsive potential due to the electrons accumulated on the PI.[1]

The morphology analysis of the surface of the operated SDBDs of PI dielectric was performed by using a secondary electron microscope (SEM), which makes it possible to observe specific PI erosion phenomena caused by O_2^+ and oxygen atom created from the accumulated electrons on the PI at a high spatial resolution (~0.1 μm). However, it is only effective when the residence time of the charges momentarily present on the surface for chemical reaction is longer than the reaction time with the dielectric surface. This work presents the experimental confirmation of the cathode layer by Paschen's law in an atmospheric AC flexible surface dielectric barrier discharge using the proposed visual diagnosis method.

[a)]Author to whom correspondence should be addressed: hysleeper@hanyang.ac.kr, Tel.: +82 2 2220 0465, Fax: +82 2 2220 1894.

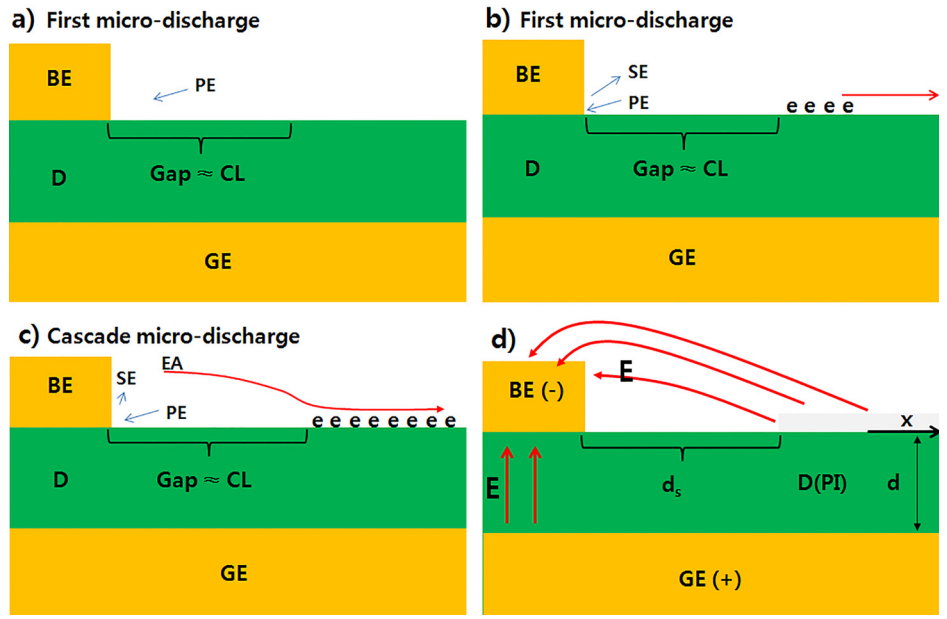

FIG. 1. Schematic drawings of the formation of the cathode layer during the first phase of negative polarity as described by Ref. 1 [i.e., side views of the discharges with relevant structures of the SDBD. This dielectric is composed of polyimide (PI) in our experiment.]. The red line with the arrow indicates the trajectory of the micro-discharges, "e" indicates the accumulated electrons on the dielectric surface. (a) The electric field line (E-line) is formed due to the potential applied to the BE. (b) The first discharges: due to the avalanches of electrons (EA), the positive ions are bombarded on the BE; then, the secondary electrons start being accelerated. (c) The surface charged layer (SCL) on the dielectric is formed (cascade microdischarges). (d) Formation of the electric field (E) line and SCL. BE = biased electrode, D = dielectric, GE = ground electrode, PE = positive ions, CL = cathode layer, SE = secondary electrons, EA = electron avalanche, and d = dielectric thickness.

For this work, sputtered-type flexible copper clad laminates (FCCL)[22] out of three types of FCCL (casting, laminating with adhesive, and sputtered)[22–24] was used as the basic material due to its ultra-fine polyimide surface,[22] which consists of a copper layer with a thickness of 8.6 μm, polyimide (Kapton ENA, $\varepsilon_R = 3.2$, ε_R has a relative permittivity) with a thickness of 38 μm, and a thin nickel-chrome layer with a thickness of 0.02 μm. The high voltage electrode with the shape of a narrow strip (18 × 118 mm^2) was formed by wet etching the copper layer. Then, an adhesive copper tape as the ground electrode was attached on the reverse side of the polyimide and laminated. Figure 2(a) shows the schematics of the experiments. The SDBD was operated at different discharging times for 1, 2, and 3 min with a fixed voltage of 2.5 kV, and a fixed frequency of 16.6 kHz. Figure 2(b) is the voltage-current waveform measured during the discharge showing a cascade of micro-discharges.[1,11] Higher current peaks during the positive voltage phase than that of the negative one are due to the longer discharge channel.[2]

The narrow etched polyimide stripes near the bottom edge of the BE, the non-etched, and then the etched polyimide areas can be observed from right to left in Figs. 3(b)–3(d). The width of the lines increases but that of the non-etched areas decreases with discharge time. Because the electric field at the bottom edge of the BE is the strongest,[25] positive ions such as O_2^+, O_4^+, N_2^+, and N_4^+ created by the electron avalanche are concentrated intensively near the bottom edge with a vacant space between the BE and the surface charged layer.[1,8] It can be concluded that the positive oxygen ions (O_2^+) mainly contribute to causing the narrow etched polyimide lines near the bottom edge of the BE.[13,14] The previous simulation results have described the distribution of the positive ions and the secondary electrons near the edge of the BE as being similar to those in the "normal cathode layer" in the SDBD models, as shown in Fig. 1(c).[1,7,8,11] Zhang *et al*. reported that a brighter luminous discharge in a higher region of the BE in an atmospheric argon SDBD is caused by more secondary electron emission from metallic electrode by positive ion bombardment.[26] The

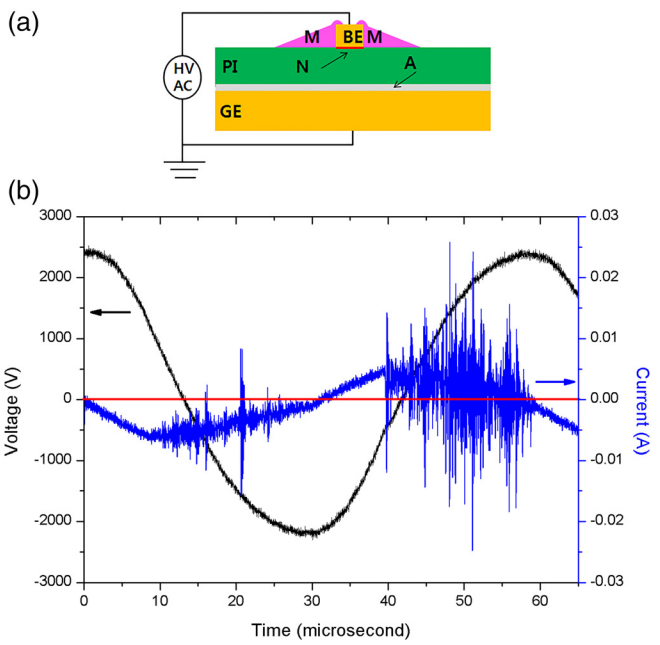

FIG. 2. (a) A schematic view of the experiment: BE: biased electrode (orange); M: micro-discharge (pink); N: Nickel-Chrome layer (red); PI: polyimide (dark green); A: adhesive layer (gray); GE: ground electrode (orange); HV AC: high voltage AC; (b) measured voltage-current waveform.

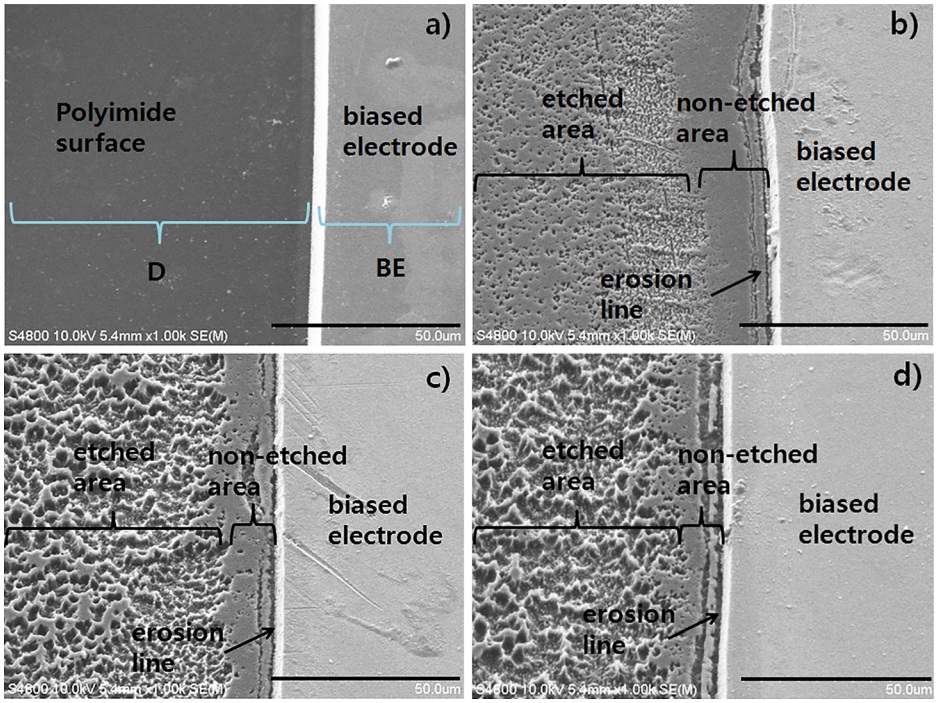

FIG. 3. Top views of the electron microscope images of dielectric surface erosion with the time duration (T_D) of discharge. (a) $T_D = 0$, (b) $T_D = 1$ min, (c) $T_D = 2$ min, (d) $T_D = 3$ min. The scale bars correspond to 50 μm.

observed polyimide erosion lines could be the experimental evidence of the cathode layer properties, as well as the bombardment of the positive ions on a BE in an atmospheric SDBD.[1,8,12,26]

As shown in Fig. 3(b), a non-etched polyimide surface with a width of about 18 μm from the lower edge of BE to the etched dielectric is experimental verification of the atmospheric AC SDBD model in Ref. 1 because the non-etched polyimide surfaces indicate no contact of micro-discharges with the surface, as shown in Fig. 1(c). In his work, the first micro-discharge along the E line contacts the dielectric surface, which is far from the vertical wall of the BE of about 20 μm, and the trajectory of the E line is formed between the surface charges on the dielectric and BE edge.[1,12] Then, the gap forms.[1,12] Electrical breakdown, hence the E line, starts from the top corner of the BE and stops at the point of the dielectric surface where the surface charge layer (SCL) starts. The distance is about 20 μm at 1 atm at 2 kV.[1,12] In this model, the length of the gap does not depend on the dielectric parameters such as the thickness (d) and relative permittivity (ε_R). It is nearly equal to the length of the cathode layer called "the gap" with a thickness of d_s, according to Paschen's law, $d_s = \left(\frac{e}{Ap}\right) ln(1 + 1/\gamma_{se})$, where p is the pressure in Torr, d_s is the cathode layer thickness in cm, e is 2.178, A is 7.5 $cm^{-1} Torr^{-1}$ for SDBDs,[1] and $\gamma_{se} \approx 0.01$ is the coefficient of the secondary electron emission.[1,26] Due to the continuous erosion of the polyimide by the reactive oxygen species created during the micro-discharges, the width of the non-etched surface decreased with the discharge time as shown in Figs. 3(a)–3(d). The cathode layer thickness, d_s, is nearly 22 μm in ambient air at 1 atm, and it has a good agreement with the length of the non-etched surface by the first micro-discharge that was deduced by the observed lengths of the non-etched surface operated for 1, 2, and 3 min, as shown in Fig. 4.

Since the height of BE (8.6 μm) is lower than the streamer distance (≈30 μm) from the dielectric surface during the phase of positive voltage,[26,27] the electrons in the streamers terminate to the top corner edge of BE,[1,6,12,27] but almost all the positive ions inside the streamers are repelled above the dielectric surface of the cathode layer.[7] Our observation suggests that the positive ions cannot penetrate the curved blocking electric field lines between the BE edge and the SCL formed on the dielectric with a gap distance (d_s) of 20 μm or so.[1,7,12] Instead, these positive ions follow the electric field lines bombarding the surface of the dielectric and causing the etching lines.

During the positive voltage, oxygen atoms are created in the head of the streamer where the distance from the PI surface is about 30 μm.[27] They do not etch the PI because most

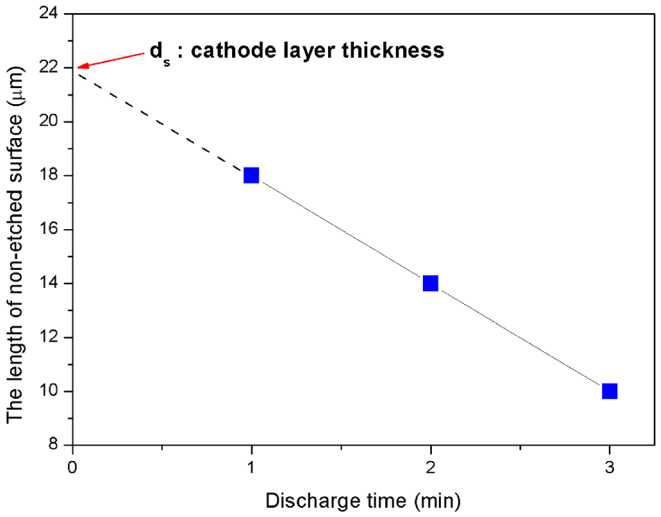

FIG. 4. Observed length of the non-etched surface as a function of the discharge time (1, 2, 3 min). The red arrow indicates the cathode layer thickness (d_s) in the first micro-discharge for the negative voltage phase.

of them immediately take part in the formation of O_3 and O_2^* [16,21] and diffusion time constant of O and O_3 is around 1 ms.[21] At 16.6 kHz, the diffusion time is longer for reaching the PI. When the polarity changes, O^{2-} and O^{3-} form by electron-attachment before reaching the PI and become the body force for thrust.[1]

In conclusion, by using the proposed visual diagnosis method with a micronised spatial resolution for surface charge distribution in SDBDs, narrow non-etched dielectric surfaces near the BE in the AC flexible SDBDs were experimentally observed at a length of 22 μm. This occurred, regardless of the three operating durations, which was in a good agreement with the length of the cathode layer according to Paschen's law.

This work was supported by the R&D Program for Technology Upgrade through R&D Performance Management System funded by the Ministry of Science and ICT of Korea.

[1]V. R. Soloviev, J. Phys. D: Appl. Phys. **45**, 025205 (2012).
[2]V. I. Gibalov and G. J. Pietsch, J. Phys. D: Appl. Phys. **33**, 2618–2636 (2000).
[3]V. R. Soloviev, A. M. Konchakov, V. M. Krivtsov, and N. L. Aleksandrov, Plasma Phys. Rep. **34**, 594–608 (2008).
[4]T. C. Corke, C. L. Enloe, and S. P. Wilkinson, Annu. Rev. Fluid Mech. **42**, 505–529 (2010).
[5]J. Pons, E. Moreau, and G. Touchard, J. Phys. D: Appl. Phys. **38**, 3635–3642 (2005).
[6]J. P. Boeuf, Y. Lagmich, T. Unfer, T. Callegari, and L. C. Pitchford, J. Phys. D: Appl. Phys. **40**, 652–662 (2007).
[7]V. R. Soloviev and V. M. Krivtsov, J. Phys. D: Appl. Phys. **42**, 125208 (2009).
[8]V. I. Gibalov, I. S. Tkachenko, and V. V. Lunin, Russ. J. Phys. Chem. A **82**, 1020–1023 (2008).
[9]G. Tathiri, E. Esmaeilzadeh, S. M. Mirsajedi, and H. M. Moghaddam, J. Appl. Fluid Mech. **7**, 525–534 (2014).
[10]S. A. Stepanyan, A. Y. Starikovskiy, N. A. Popov, and S. M. Starikkovskaia, Plasma Sources Sci. Technol. **23**, 045003 (2014).
[11]V. I. Gibalov and G. J. Pietsch, Plasma Sources Sci. Technol. **21**, 024010 (2012).
[12]V. R. Soloviev, I. B. Selivonin, and I. A. Moralev, Phys. Plasmas **24**, 103528 (2017).
[13]C. H. Steinbrüchel, B. J. Curtis, H. W. Lehmann, and R. Widmer, IEEE Trans Plasma Sci. **PS-14**, 137–144 (1986).
[14]Z. Shpilman, I. Gouzman, G. Lempert, E. Grossman, and A. Hoffman, Rev. Sci. Instrum. **79**, 025106 (2008).
[15]S. K. Rutledge and J. A. Mihelcic, Surf. Coat. Technol. **39/40**, 607–615 (1989).
[16]J. Y. Jeong, S. E. Babayan, V. J. Tu, J. Park, I. Henins, R. F. Hicks, and G. S. Selwyn, Plasma Source Sci. Technol. **7**, 282–285 (1998).
[17]E. M. Anokhin, D. N. Kuzmenko, S. V. Kindysheva, V. R. Soloviev, and N. L. Aleksandrov, Plasma Source Sci. Technol. **24**, 045014 (2015).
[18]Y. B. Golubovskii, V. A. Maiorov, J. Behnke, and J. F. Behnke, J. Phys. D: Appl. Phys. **35**, 751–761 (2002).
[19]M. B. Zhelezniak, A. Kh. Mnatsakanian, and S. V. Sizykh, High Temp. **20**, 357–362 (1982).
[20]S. Vepřek and F.-A. Sarott, Plasma Chem. Plasma Process **2**, 233–246 (1982).
[21]B. Eliasson, M. Hirth, and U. Kogelschatz, J. Phys. D: Appl. Phys. **20**, 1421–1437 (1987).
[22]J. S. Eom and S. H. Kim, Thin Solid Films **516**, 4530–4534 (2008).
[23]C. Y. Lee, J. H. Lee, D. H. Choi, H. J. Lee, H. S. Kim, S. B. Jung, and W. C. Moon, Microelectron. Eng. **84**, 2653–2657 (2007).
[24]B. I. Noh, J. W. Yoon, and S. B. Jung, Int. J. Adhes. Adhes. **30**, 30–35 (2010).
[25]A. K. Srivastava and G. Prasad, Phys. Lett. A **374**, 3960–3966 (2010).
[26]R. Zhang, R. J. Zhan, X. H. Wien, and L. Wang, Plasma Source Sci. Technol. **12**, 590–596 (2003).
[27]V. R. Soloviev and V. Kristov, J. Phys.: Conf. Ser. **927**, 012059 (2017).